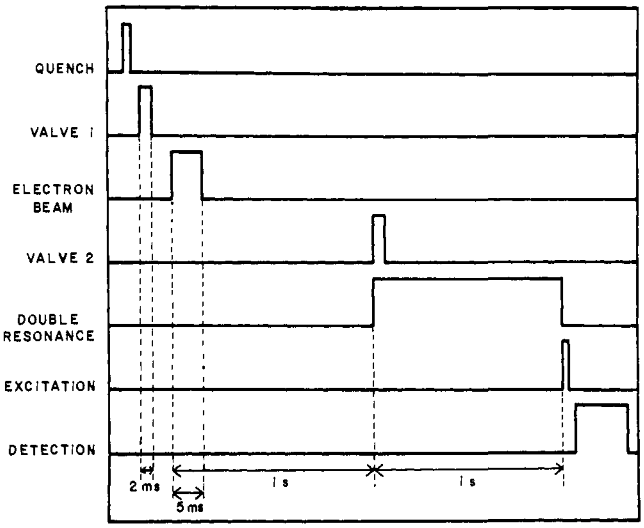

Figure 3. Sequence of events in the FTMS gas-pulsing experiments.

in the ion source. The source pressure was measured by using an ion gauge which was calibrated by a Hasting gauge mounted on a regular probe. When CS_2 was used as a charge-exchange gas, its pressure was varied in the range 0.05–0.4 torr.

The apparatus used for low-pressure ion–molecule reaction studies was a home-built FTMS[40] controlled by a Nicolet FTMS-1000 data system. The cell was located in a magnetic field of 1.2 T. The trapping voltage was to 1 V. The ions were formed by an electron beam biased at 9–15 eV and pulsed for 5 ms. The ions were excited by a 800-kHz excitation bandwidth "chirp" and measured by acquiring the mass spectrum over the mass range 20–150 amu at variable time delays ranging from 1 to 700 ms. Double-resonance pulses were set for continuous ejection of the ions of interest throughout the reaction period. The reactants (1:1) at a total pressure of 1×10^{-6} torr were introduced into the cell through metal inlets maintained at ambient temperature.

The consecutive reactions in the FTMS were performed by using a pulsed reagent inlet technique. The pulsed valve inlet setup has been described in detail previously[35] and will not be discussed here. The C_5H_8 hydrocarbons were admitted into the cell to a static pressure of 4×10^{-8} torr as described above. The experimental sequence is shown in Figure 3. Benzene, used as a charge-exchange reagent, was admitted via a pulse of 2-ms duration. The second valve pulse was delayed 1 s from the first pulse in order to allow thorough removal of the excess neutral reagent. Detection was then delayed 1 s in order to permit adequate time for reaction of the stored ions and the neutral reagent. The reagents were introduced to the valves from stainless steel reservoirs at 0.5–1 torr, producing pressure pulses with a maximum amplitude of 3×10^{-6} torr in the vacuum chamber containing the cell.

1-Methylcyclobutene was synthesized by isomerization of methylenecyclobutane by using the procedure of Shabtai and Gil-Av.[41] The reaction was conducted over freshly prepared Na/alumina catalyst at 2–3 °C. Methylenecyclobutane was freshly distilled over sodium metal under vacuum. The product was purified by preparative GC by using a 4 m × 6 mm stainless steel column packed with 20% TCEP coated on 60/80 Chromosorb (Supelco). The column was operated at ambient temperature with the injector and detector at 60 °C. When He was used as a carried gas at a flow rate of 22 mL min^{-1}, the 1-MCB emerged from the column at 11.0 min and the unreacted methylenecyclobutane at 14.4 min.

3-Methylcyclobutene was prepared by a photochemical-induced isomerization of *trans*-1,3-pentadiene (99%) according to the procedure of Frey[5a] except cyclohexane was used as a solvent in place of *n*-hexane and isopentane was not added to the reaction mixture. *n*-Hexane interfered with the purification of 3-MCB when the above-mentioned GC method was used.

All other chemicals were purchased from commercial sources (Wiley Organics) as >99% purity grade and used without further purification.

Acknowledgment. This work was supported by the National Science Foundation (Grant CHE-8320388) and by the Midwest Center for Mass Spectrometry, a National Science Foundation Regional Instrumentation Facility (Grant CHE-82-11164).

Registry No. 1-Methylcyclobutene radical cation, 91631-62-8; 3-methylcyclobutene radical cation, 91738-63-5; isoprene radical cation, 50535-53-0; (*E*)-1,3-pentadiene radical cation, 84847-89-2; 1,4-pentadiene radical cation, 91631-63-9; cyclopentene radical cation, 34512-37-3; methylenecyclobutane radical cation, 91631-64-0; 1-pentyne radical cation, 77742-02-0; 2-pentyne radical cation, 91631-65-1.

---

(40) Ledford, E. B., Jr.; Ghaderi, S.; White, R. L.; Spencer, R. B.; Kulkarni, P. S.; Wilkins, C. L.; Gross, M. L. *Anal. Chem.* **1980**, *52*, 463.

(41) Shabtai, J.; Gil-Av, E. *J. Org. Chem.* **1963**, *28*, 2893.

Molecular Dynamics Study of Solvation in Urea–Water Solution

Robert A. Kuharski and Peter J. Rossky*

Contribution from the Department of Chemistry, University of Texas, Austin, Texas 78712.
Received December 21, 1983

Abstract: In order to study the effect of urea on water structure, a molecular dynamics simulation of a dilute aqueous urea solution has been carried out. A rigid body model is used to represent urea, and the intermolecular potentials are given by Lennard-Jones and electrostatic terms. Only very small differences are observed between the properties of water molecules in the solvation region of urea and the bulk, and these differences can be assigned to direct urea–water interactions, with no substantial perturbation of water–water interactions. Implications for the mechanism of solubilization of hydrocarbons by urea are discussed.

I. Introduction

Aqueous urea solutions have interesting and anomalous properties. Urea forms nearly ideal mixtures with water.[1] Yet, is a strong protein denaturant,[2] increases the solubility of hydrocarbons,[3] and inhibits micellar aggregation.[4] Due in large part to this protein denaturing ability, aqueous urea solutions have been studied extensively. In spite of this, the mechanism by which urea acts remains unresolved.

---

(1) Stokes, R. H. *Aust. J. Chem.* **1967**, *20*, 2087.

(2) Brandts, J. F.; Hunt, L. *J. Am. Chem. Soc.* **1967**, *89*, 4826.

(3) Wetlaufer, D. B.; Malik, S. K.; Stoller, L.; Coffin, R. I *J. Am. Chem. Soc.* **1964**, *86*, 508.

(4) Shick, M. J. *J. Phys. Chem.* **1964**, *68*, 3585.

0002-7863/84/1506-5786$01.50/0

Hydrophobic interactions play an important role in the conformation of proteins and nucleic acids. Accordingly much of the discussion on urea has centered around its potential ability to weaken these interactions. We will also focus on urea's role in hydrophobic phenomena. In doing this, we are not implying that urea's interactions with polar groups is not essential for the denaturation process.[5,6] The *ability* of the denaturant to solvate the peptide group appears to be an important characteristic.[6] However, the influence on apolar groups is also important, and perhaps dominant.[5,6] It is the *molecular* description of solvation in aqueous urea solutions that is of central interest here. A clear molecular description of pure water structure[7,8] as well as hydrophobic hydration[9-11] and the hydrophobic interaction[12,13] is emerging from computer simulations, and the determination of how a molecule like urea alters this description is a logical next step.

The idea that urea's denaturing ability was due at least in part to a weakening of hydrophobic interactions gained impetus from the work of Wetlaufer et al.[14] By measuring the solubilities of a group of hydrocarbons in water and aqueous urea they found that, with the exception of methane and ethane, urea increased the solubilities of the hydrocarbons tested, and the transfer of hydrocarbons from water to aqueous urea was characterized by positive changes in both enthalpy and entropy. In discussing the mechanism by which urea acted, they were able to rule out solvation solely by urea due to the approximately linear dependence of solubility on urea concentration and proposed two plausible mechanisms: (*1*) an indirect mechanism where urea alters the "structure" of water in a way that facilitates solvation of a hydrocarbon by water molecules and (2) a direct mechanism where the hydrocarbons are solvated by both urea and water molecules. There have also been attempts to explain the properties of aqueous urea solutions with urea association models.[1,15] However, such an interpretation appears inconsistent with both the linear dependence of solubility on urea concentration and NMR[16] and ultrasonic attenuation experiments,[17] so we do not consider it further here.

Interest in the indirect mechanism has led to numerous experiments on the effect of urea on water structure. Many of the results have indicated that urea decreases the structure of water.[16-25] Examples include upfield shift in NMR water proton resonances,[16] decrease in shear and structural contributions to ultrasonic absorption,[17] and an increase in absorption in the IR band associated with the stretching of "free" OH.[18] These have been viewed by some as supporting the indirect mechanism.

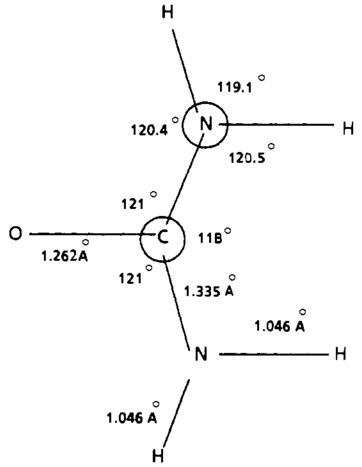

Figure 1. Urea Crystal Structure.

There are, however, several objections to this conclusion. First, there are also experimental results which indicate that urea has no appreciable effect on water structure, e.g., no change in O–D stretching frequency for HDO[26] and positive partial molal heat capacity of urea in water.[27] However, of most importance, the classification of urea as a "structure breaker" through the cited experimental results does not appear firmly connected to the solution phenomena discussed above. In particular, the observed effects on water are often less than for other solutes which are so classified, and, further, no correlation has been established between a solutes "structure breaking" tendency and either protein denaturation or hydrocarbon solubilization.[24,28] These inconsistencies have been pointed out by several authors[29,30] who emphasized that great care must be exercised in attempting to attribute solution properties to the structure making or structure breaking effects of a solute.

From this discussion, it is clear that a better understanding of aqueous urea solutions on the molecular level is necessary to evaluate the indirect mechanism. It is the molecular description of this potential mechanism that we address here.

Computer simulations have been very successful in elucidating the molecular description of aqueous systems.[11,31,32] In this paper, we apply this technique using a model solute which we believe contains the essential features necessary to describe urea and its interactions with water. We report on a molecular dynamics simulation of this model solute in ST2[7] water. The results of a corresponding simulation, but of a ternary system in which an apolar sphere is included, are presented in a separate paper.

II. Model Solution

In this section we describe the elements of the model simulated.

A. Geometry and Intramolecular Potential of Urea. The geometry of urea, obtained from crystal data,[33] is shown in Figure 1. As indicated, the molecule is planar in the crystal. Nevertheless, in solution one must consider the possibility that the hydrogens may bend out of plane. If this bending resulted in a significant stabilization of a solute solvation site it would be a factor in the solvation of urea and would be important in the model. The relevance here is the proton accepting capability of urea nitrogen.

Although the appropriate studies have not been done for urea, formamide, a closely related molecule, has been studied extensively, and the results serve as a useful guide to estimating the likelihood and importance of this bending in urea. The microwave spectrum[34] along with quantum calculations[35,36] indicate that the potential

---

(5) Enea, O.; Jolicoeur, C. *J. Phys. Chem.* **1982**, *86*, 3870.

(6) Franks, F. In "Water, A Comprehensive Treatise"; Franks, F., Ed.; Plenum Press: New York, 1975, Vol. 4, Chapter 1, p 85.

(7) Stillinger, F. H.; Rahman, A. *J. Chem. Phys.* **1974**, *60*, 1545.

(8) Mezei, M.; Beveridge, D. L. *J. Chem. Phys.* **1981**, *74*, 622.

(9) Owicki, J. C.; Scheraga, H. A. *J. Am. Chem. Soc.* **1977**, *99*, 7413.

(10) Swaminathan, S.; Harrison, S. W.; Beveridge, D. L. *J. Am. Chem. Soc.* **1978**, *100*, 3705.

(11) Rossky, P. J.; Karplus, M. *J. Am. Chem. Soc.* **1979**, *101*, 1913.

(12) Geiger, A.; Rahman, A.; Stillinger, F. H. *J. Chem. Phys.* **1979**, *70*, 263.

(13) Pangali, C.; Rao, M.; Berne, B. J. *J. Chem. Phys.* **1979**, *71*, 2975.

(14) Wetlaufer, D. B.; Malik, S. K.; Stoller, L.; Coffin, R. L. *J. Am. Chem. Soc.* **1964**, *86*, 509.

(15) Kresheck, G. C.; Scheraga, H. A. *J. Phys. Chem.* **1965**, *69*, 1704.

(16) Finer, E. G.; Franks, F.; Tait, M. J. *J. Am. Chem. Soc.* **1972**, *94*, 4424.

(17) Hammes, G. G.; Schimmel, P. R. *J. Am. Chem. Soc.* **1967**, *89*, 442.

(18) Dwek, R. A.; Luz, Z.; Shpores, M. *J. Phys. Chem.* **1970**, *74*, 2230.

(19) Walrafren, G. E. *J. Chem. Phys.* **1966**, *44*, 3726.

(20) Vidulich, G. A.; Gleason, F. X.; Lynch, J. F.; Mattern, W. C.; McCabe, R. *Sol. Chem.* **1972**, *1*, 263.

(21) Khamova, V. I.; Ponomareva, A. M.; Mischenko, K. P. *Russ. J. Phys. Chem.* (*Engl. Transl.*) **1966**, *40*, 748.

(22) MacDonald, J. C.; Serphillips, J.; Guerreva, J. J. *J. Phys. Chem.* **1973**, *77*, 370.

(23) Philip, P. R.; Perron, G.; Desnoyers, J. E. *Can. J. Chem.* **1974**, *52*, 1709.

(24) Bonner, O. D.; Bednarek, J. M.; Arisman, R. K. *J. Am. Chem. Soc.* **1977**, *99*, 2848.

(25) Rupley, J. A. *J. Phys. Chem.* **1964**, *68*, 2002.

(26) Swenson, C. A. *Arch. Biochem. Biophys.* **1966**, *117*, 494.

(27) Subramanian, S.; Balasubramanian, D.; Ahluwalia, J. C. *J. Phys. Chem.* **1969**, *73*, 266.

(28) Jencks, W. P. *Fed. Suppl.* **1965**, *24*, S-50.

(29) Holtzer, A.; Emerson, M. F. *J. Phys. Chem.* **1969**, *73*, 26.

(30) Roseman, M.; Jencks, W. P. *J. Am. Chem. Soc.* **1975**, *97*, 631.

(31) Mehrotia, P. K.; Beveridge, D. L. *J. Am. Chem. Soc.* **1980**, *101*, 4287.

(32) Geiger, A. *Ber. Bunsenges. Phys. Chem.* **1981**, *85*, 52.

(33) Andrew, E. R.; Hyndman, D. *Discuss. Faraday Soc.* **1955**, *19*, 195.

(34) Hirota, E.; Sugisaki, R.; Neilsen, C. J.; Sorensen, G. O. *J. Mol. Spectrosc.* **1974**, *49*, 251.

Table I. Parameters for Model I

atom	q, e	ϵ, kcal/mol	σ, Å
C	0.633	0.0900	3.208
O	−0.443	0.2304	2.640
N	−0.448	0.1600	2.770
H_C	0.188	0.004489	1.604
H_T	0.165	0.004489	1.604

well for bending the hydrogens is very flat in the vicinity of the planar structure. However, the out-of-plane solvation site has given only small binding energies, compared to other sites, in quantum calculations on formamide–water dimers for both the planar formamide geometry and that with the hydrogens bent away from the water.[37,38] A corresponding calculation for this site for a urea–water dimer,[39] without hydrogen distortion, showed even less binding energy than the corresponding formamide–water calculation, utilizing the same basis set.[38]

These results indicate this proton bending should not significantly effect the description of urea solvation. Hence, a rigid body model for the solute should be adequate for a study of this aspect of solution structure. In the present simulation, urea is constrained to the geometry of Figure 1.

B. Urea–Water Potential. The knowledge of urea–water interactions is limited. The most important interactions here are clearly hydrogen bonds between water and the C=O and NH_2 groups of urea. Experimental results for urea solutions are consistent with the view that urea–water and water–water hydrogen bonds are of "similar" strength.[16,23,26] Quantum mechanical calculations on formamide–water dimers[37,40–42] also indicate similar strengths for these types of hydrogen bonds (within about 1.5 kcal/mol) and provide information on the shape of the interaction potential. The implications of such calculations for hydrogen bond potentials have been discussed previously.[43]

Obviously there are wide ranges of potentials that are consistent with this limited knowledge of the interactions. Potentials of the form

$$V_{ij} = \frac{A_{ij}}{r_{ij}^{12}} - \frac{B_{ij}}{r_{ij}^{6}} + \frac{C_{ij}}{r_{ij}} \tag{1}$$

where V_{ij} is the potential between sites i and j, r_{ij} is the distance between the sites, and A_{ij}, B_{ij}, and C_{ij} are parameters of the interaction, have been shown to give good fits to quantum calculations for a wide range of species[38,44] and are frequently used in computer simulations. We have considered in detail two reasonable sources for the urea–water interaction parameters, and we discuss these below.

In model I, the ST2 potential parameters[7] are used for water, and the interaction between a water molecule and urea is given by

$$V_{\mathrm{wu}} = \sum_{\lambda=1}^{8} \left\{ 4\sqrt{\epsilon_{\mathrm{w}}\epsilon_{\lambda}} \left[\left(\frac{\bar{\sigma}_{\lambda}}{r_{\mathrm{O}\lambda}}\right)^{12} - \left(\frac{\bar{\sigma}_{\lambda}}{r_{\mathrm{O}\lambda}}\right)^{6} \right] + \sum_{j=1}^{4} \frac{q_j q_{\lambda}}{r_{j\lambda}} \right\} \tag{2}$$

where λ indexes the atoms in urea, O is the oxygen atom in water, and j indexes the four point charges in ST2 water. ϵ and σ are Lennard-Jones parameters, with $\bar{\sigma}_{\lambda} = (1/2)(\sigma_{\mathrm{w}} + \sigma_{\lambda})$, and q is the site electrostatic charge. The charges on the urea atoms are taken from a Mulliken population analysis of urea.[45] The Lennard-Jones parameters for the urea atoms are taken to be the same as those used in a previous model for peptides.[43] Table I contains the values of the parameters used for urea.

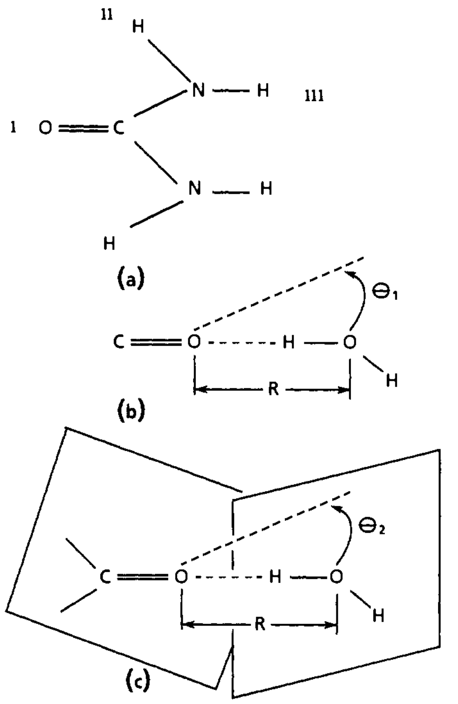

Figure 2. Three distinct hydrogen bonding sites of urea and geometric parameters used to describe urea–water hydrogen bonding.

Model II is based on the pair potentials for the interaction of amino acids with water developed by Clementi et al.[44] The interaction between a water molecule and urea is given by (cf. eq 2)

$$V_{\mathrm{wu}} = \sum_{\lambda=1}^{8} \sum_{j=1}^{3} \left[-\frac{A_{\lambda j}}{r_{\lambda j}^{6}} + \frac{B_{\lambda j}}{r_{\lambda j}^{12}} + \frac{C_{\lambda j} q_{\lambda} q_j}{r_{\lambda j}} \right] \tag{3}$$

where λ again indexes the atoms in urea and j indexes the sites in water. Although calculations were not done on urea, the atoms in urea can unambiguously be assigned to the 23 classes they developed, which assign the coefficients $A_{\lambda j}$, $B_{\lambda j}$, and $C_{\lambda j}$. The water molecule of ref 44 was used, and the charges on the urea atoms were estimated from their work as follows. Initially the charges of the CONH2 group of asparagine in ref 44 are taken and then the effect of replacing the remainder of the asparagine molecule with an NH_2 is estimated. This estimation was made by taking the ratio of the charges on C, O, N, and H in urea and acetamide in ref 45, obtained from CNDO/2, and multiplying the charges from asparagine by these ratios. The values of the parameters of model II are listed in Table II.

To compare the two models we look at the three distinct hydrogen bonding sites on urea. These sites are shown in Figure 2 along with the parameters used to describe the orientation. The radial and angular dependence of the potentials for the two models have the same qualitative features and are consistent with the formamide–water calculations. That is, the energy varies fairly rapidly with distance but not with the angles in the vicinity of the minimum.

The minimum energies and the angles θ_1 of the minima for both models are listed in Table III. The energies for model I are all reasonably close to the minimum for ST2 water (6.8 kcal/mol). The bond to C=O is the strongest, and the difference between the strongest and weakest bonds is 1.1 kcal/mol. In model II the

---

(35) Carlsen, N. R.; Random, L.; Riggs, N. V.; Rodwell, W. R. *J. Am. Chem. Soc.* **1979**, *101*, 2233.

(36) Malon, P.; Bystricky, S.; Blaha, K. *Collect. Czech. Chem. Commun.* **1978**, 781.

(37) Johansson, A.; Kollman, P.; Rothenberg, S.; McKelvey, J. *J. Am. Chem. Soc.* **1974**, *96*, 3794.

(38) Algona, G.; Pullman, A.; Scroco, E.; Tomusi, J. *Int. J. Pept. Protein Res.* **1973**, *5*, 251.

(39) Orita, Y.; Pullman, A. *Theoret. Chim. Acta* **1977**, *45*, 257.

(40) Hinton, J. F.; Harpool, R. D. *J. Am. Chem. Soc.* **1977**, *99*, 349.

(41) DelBene, J. E. *J. Am. Chem. Soc.* **1978**, *100*, 1387.

(42) DelBene, J. E. *J. Chem. Phys.* **1975**, *62*, 1961.

(43) Rossky, P. J.; Karplus, M.; Rahman, A. *Biopolymers* **1979**, *18*, 825.

(44) Clementi, E.; Cavallone, F.; Scordamaglia, R. *J. Am. Chem. Soc.* **1977**, *99*, 5531; **1977**, *99*, 5545.

(45) McGuire, R. F.; Momany, F. A.; Scheraga, H. A. *J. Phys. Chem.* **1972**, *76*, 375. Charges for urea in Figure 1 do not give a neutal molecule. To achieve neutrality the charge on C was changed to 0.633.

Table II. Parameters for Model II[a]

atom	q, e	class	A_O	B_O	C_O	A_H	B_H	C_H
C	0.58	5	0.24269627×10^3	0.570163312×10^4	0.998202369	0.356004411×10^1	0.184585125×10^6	0.999759927
O	−0.48	10	0.102073144×10^2	0.2651569141×10^6	1.00092629	0.163284536×10^3	0.762464880×10^4	0.999389425
N	−0.67	13	0.3183200038×10^3	0.615968625×10^6	1.00005582	0.347660562×10^1	0.682350397×10^4	1.00299819
H_C	0.31	1	0.227048409×10^3	0.3194285464×10^4	0.998202369	0.207521847×10^1	0.173850511×10^4	1.00088759
H_T	0.31	1	0.227048409×10^3	0.3194285464×10^4	0.998202369	0.207521847×10^1	0.173850511×10^4	1.00088759

[a] Classes defined in ref 11; energies in kcal/mol for distances in angstroms; A_O is interaction with O on water, A_H is interaction with H on water, etc.

Table III. Minimum Energies and Geometries

	model I[a]			model II		
	energy, kcal/mol	R_{x-y}, Å	θ_1, deg	energy	R_{x-y}, Å	θ_1, deg
H bond I	−6.5	2.55	−74	−5.2	3.01	69
H bond II	−5.4	2.94	24	−8.9	2.79	−25
H bond III	−5.9	2.89	23	−7.5	2.84	0

[a] Used in simulation reported here.

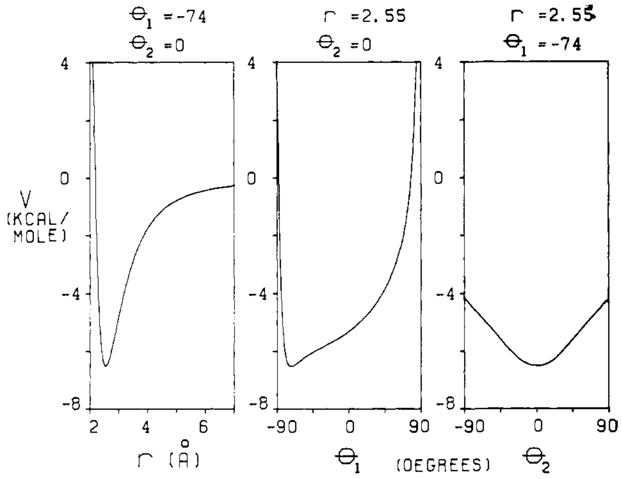

Figure 3. Urea–water hydrogen bond I potential surface.

C=O bond is the weakest, and the difference between the strongest and weakest bonds is 3.7 kcal/mol.

In deciding between the models, there are several ab initio SCF calculations using the minimal STO-3G basis set on the formamide–water dimers,[37,40–42] and we can use these guidance. There is some disagreement on which bond is the strongest, but the difference between strongest calculated hydrogen bond energy (7.6 kcal/mol) and the weakest (6.4 kcal/mol) is rather small, only 1.2 kcal/mol. The values for model I are closer to these calculations than model II, and on this basis we chose model I for the simulation.

Figures 3–5 contain the urea–water potential energy curves as functions of the distances R_{xy} in the bond x–H...y, θ_1 and θ_2 for model I. The curves show the expected radial and angular dependence (cf. ref 43). The angular curves are relatively flat over a wide range of angles then rise steeply due to overlap of the Lennard-Jones spheres. We have also examined the out-of-plane site mentioned in the preceding section. The minimum energy is −1.4 kcal/mol compared to −1.1 kcal/mol in the quantum calculation of the urea–water dimer.[39] Furthermore, bending urea's hydrogens 20° out of the plane results in only a 0.4 kcal/mol stabilization of this site, further supporting the rigid body model used.

III. Results

A. Simulation Procedure. The initial configuration for the simulation was obtained by taking the final configuration of an ST2 water simulation of 216 molecules, placing the urea molecule in the center, and removing the waters with close contacts. The simulated sample contains 210 water molecules and 1 urea molecule, corresponding to an apparent urea "concentration" of 0.26 M. The sample is contained in a cube of length 18.50 Å to give the experimental density (1.0024 g/mL for 0.26 M urea at 298 K).[46]

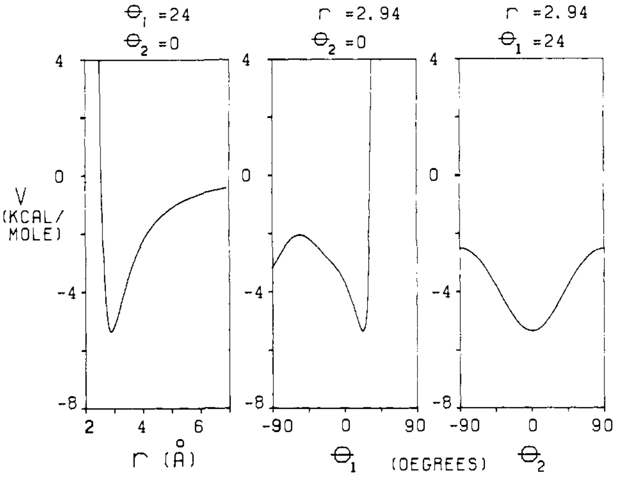

Figure 4. Urea–water hydrogen bond II potential surface.

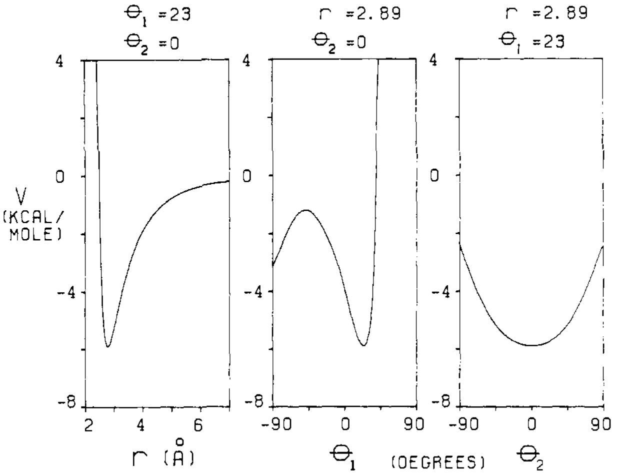

Figure 5. Urea–water hydrogen bond III potential surface.

As in other simulations periodic boundary conditions are used, and the interactions between molecules are cut off at a finite distance. If the distance between the centers of mass of two water molecules is larger than 8.0 Å they do not interact. Urea–water interactions are included only if the distance between the center of mass of the water and the center of charge of urea is less than 8.0 Å. This was done to ensure that every water molecule that interacts with urea feels the potential from the entire urea molecule.

The equations of motion were numerically integrated by using the Verlet algorithm[47] with a time step of 1×10^{-15} s. The ST2 water geometry was maintained with subroutine SHAKE.[48] Since the SHAKE algorithm is singular for strictly planar systems, we used the quaternion algorithm of Evans[49] to calculate the solute

---

(46) Gucher, F. T. Jr.; Gage, G. W.; Moser, G. E. *J. Am. Chem. Soc.* **1938**, *60*, 2582.

(47) Verlet, L. *Phys. Rev.* **159**, 184 (1967).

(48) Ryckaert, J. P.; Ciccotti, G.; Berendsen, H. J. C. *J. Comput. Phys.* **1977**, *23*, 327.

(49) Evans, D. J.; Murad. S. *Mol. Phys.* **1977**, *34*, 327.

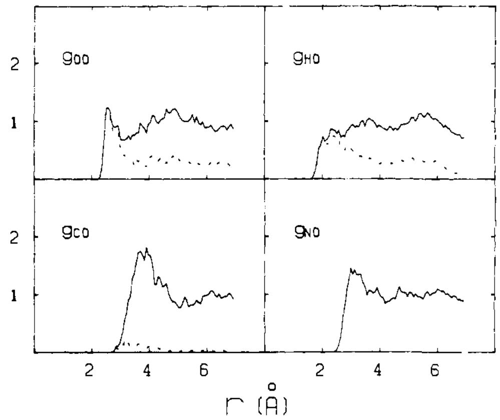

Figure 6. Urea atom–water oxygen radial distributions functions: total (—), primary (---). See text for definitions.

dynamics, maintaining the geometry of Figure 1.

The sample was equilibrated for a period of 18 900 steps. During the equilibration period the velocities were periodically replaced with a random Boltzmann distribution to ensure thermal equilibrium in the sample. After the equilibration, a 10 000-step or 10-ps simulation was run for analysis. The average water rotational and translational temperatures were both 299 K. To test the important requirement that the waters immediately surrounding urea were in thermal equilibrium with the bulk, every 200 steps the average temperature, over the preceding 200 steps, of the waters whose center of mass was within 6 Å of the urea center of charge was determined. This region included 25–30 waters. The average of this local temperature over the simulation was 298 K indicating that excellent thermal equilibrium was achieved. The average temperature for the single urea molecule was 295 K.

B. Structural Analysis. Those who maintain urea is a water "structure breaker" generally contend that urea acts to disrupt water–water interactions.[16,24,50] Accordingly, in analyzing the simulation results, wherever possible we will attempt to separate those effects which can be attributed solely to direct interactions between urea and water and those which are manifestations of urea-induced changes in water–water interactions.

1. Definition of the Solvation Shell. If urea induces a significant change in water structure, the water molecules close to urea would be expected to be the most affected. To investigate this, we separate the water molecules in the simulation into two groups, the "shell" (waters close to urea) and the "bulk" (waters not in the shell). The definition of the shell is somewhat arbitrary. If too large a shell region is chosen there will be a tendency to mask any differences between the regions. If the region chosen is too small, important contributions may be omitted. A definition roughly corresponding to the first hydration shell should meet the requirements for a meaningful comparison of the two regions.

To define the hydration shell, we calculated the urea atom water oxygen radial distribution functions and the corresponding primary radial distribution functions as described by Mehrotra and Beveridge.[31] In the so-called primary radial distribution functions, each water molecule oxygen atom is included only in the distribution corresponding to the urea atom to which it is closest. Due to the geometry of urea, only a small fraction of the water molecules are closest to carbon or nitrogen; the oxygen atoms of these solvent molecules lie in a cylinder whose axis is perpendicular to the plane of urea. We combined these into one group and assigned them to the distribution for the carbon atom.

The resulting distribution functions are shown in Figure 6. From these results, we arrive at a satisfactory definition of the urea shell: water molecules whose oxygen atom centers are within 2.75 Å of a urea hydrogen, 3.75 Å of the urea oxygen, or 4.75 Å of the urea carbon. The shell region is shown in Figure 7. The classification of a water molecule as shell or bulk in the analysis below is based on its instantaneous position in each configuration. This results in an average of 12.6 water molecules in the defined shell region and 197.4 in the bulk region.

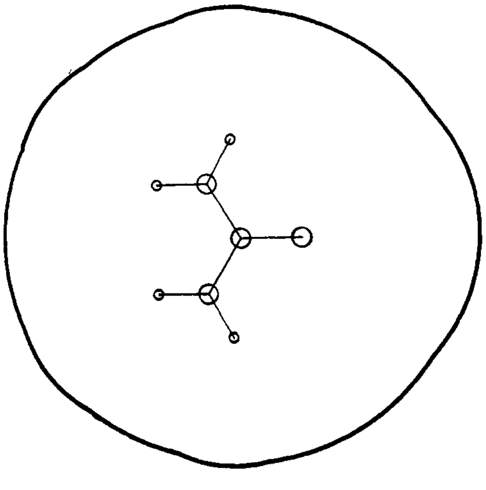

Figure 7. Boundary of defined urea shell region in the molecular plane. Note that the region appears nearly circular in this plane but is not.

Table IV. Average Binding Energies[a]

	shell	bulk
$\langle E_B^T \rangle$	−20.02	−20.04
$\langle E_B^W \rangle$	−19.14	−20.01
$\langle E_B^U \rangle$	−0.88	−0.03

[a] All values in kcal/mol.

2. Comparison of Shell and Bulk Regions. We now compare various measures of structure for the shell and bulk regions. The choice of quantities analyzed follows now fairly standard practice.[7-13] In previous simulations, comparisons of these quantities for solvation and bulk regions have been successfully used to describe both the "structure making" effect of apolar solutes[9-11] and the "structure breaking" effect of ions.[32] In evaluating the effect of urea on "water structure", the relative size of such effects compared to that of other solutes can be used as one guide.

Binding Energies. The total binding energy of a water molecule is the sum of its interaction energies with all other molecules in the system, which we denote as E_B^T. We also definie E_B^U as the interaction energy of a water molecule with urea and E_B^W as the sum of the interaction energies of a water molecule with other water molecules, so that

$$E_B^W = E_B^T - E_B^U$$

The averages of these quantities over the simulation for the shell and bulk regions are listed in Table IV. All energetic quantities are calculated by using the same potential cutoffs as in the simulation, unless indicated otherwise.

Not surprisingly, $\langle E_B^W \rangle$ is more positive for the shell region, since shell waters have fewer near-neighbor water molecules due to the presence of urea. The decrease in near-neighbor water interactions for the shell is compensated for by urea–water interactions, and the average total binding energies for the two regions are essentially identical. A shift to more positive binding energies for the shell could be taken as indicative of a structure breaking effect, and this has been observed in simulations of aqueous electrolyte solutions[32] but is absent here.

We have also calculated the distribution of total and "local" binding energies for the water molecules in the two regions. The local binding energies are defined by using a 3.5-Å cutoff for water–water interactions and including urea–water interactions only for the water molecules in the designated shell. The distributions are shown in Figure 8. The small number of molecules in the shell region leads to larger statistical noise, but there is no indication of a difference in the binding energy distributions for the two regions. Thus, there is no evidence of a structure breaking effect in either the average binding energy or binding energy distributions.

---

(50) Frank, H. S.; Franks, F. *J. Chem. Phys.* **1968**, *48*, 4746.

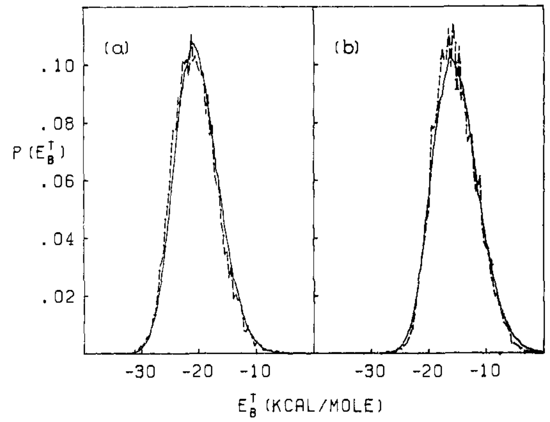

Figure 8. Distributions of water molecule binding energies: total binding energies (a), local binding energies (b), bulk (—), shell (---).

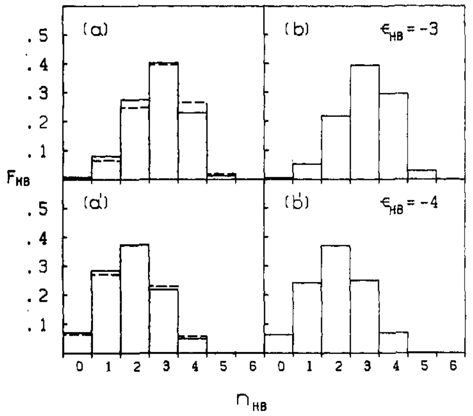

Figure 9. Fraction of water molecules participating in n_{HB} hydrogen bonds for two values of the energetic cutoff, ϵ_{HB}. Shell (a,a′), bulk (b,b′). The solid lines include only water–water bonds; the dashed lines include also urea–water bonds.

Hydrogen Bonding. The more explicit attempts to explain a structure breaking tendency for urea[16,24,50] generally propose that the water in the vicinity of urea is involved in fewer hydrogen bonds than bulk water. We now compare the hydrogen bonding characteristics of the two regions to look for evidence of such a structure breaking effect. We use an energetic definition of a hydrogen bond; two molecules are considered as hydrogen bonded if their interaction energy is less than or equal to the energetic cutoff employed. Histograms of the average fraction (F_{HB}) of water molecules in each region participating in n_{HB} hydrogen bonds are shown in Figure 9 for two values of this energetic cutoff. For the shell region we show the histograms including and excluding the urea–water hydrogen bonds. Table V contains the average number of hydrogen bonds ($\langle n_{HB} \rangle$) for the two regions for the energetic cutoffs used.

When urea–water hydrogen bonds are included there is little difference in the hydrogen bond characteristics of the two regions. There is, at most, only a slight decrease in hydrogen bonding in the shell region. Our calculations show that the shell water manifests only a 3% decrease in the numbers of hydrogen bonds, and it is difficult to justify this difference as statistically significant. In any case, it is unlikely that such a small decrease in hydrogen bonding could be assigned as the major cause of urea's solution properties.

Pair Interaction Energy Distributions. In the two preceding sections we have shown that there is no statistically significant difference in the binding energy and at most only a small difference in the hydrogen bonding characteristics of the two solvent regions. These measures of structure, however, can be deceiving. For example, the difference in these measures between the region around an apolar solute and bulk water is small, yet this region is considerably more "structured" than bulk water. It is the geometrical restrictions required in order to obtain similar binding energy and hydrogen bond characteristics that characterize the structure there. We now analyze the molecular pair interactions energy distributions to determine how the shell region attains its binding energy and hydrogen bond characteristics.

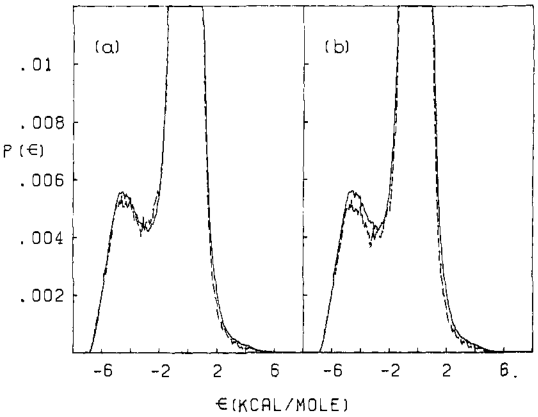

Figure 10. Normalized distributions of pair interaction energies for water molecules. In (a) water–urea interactions are included, in (b) only water–water interactions are included. Bulk (—), shell (---).

Figure 10 shows these distributions for shell and bulk molecules. In Figure 10a urea–water interactions are included while in Figure 10b they are not. These distributions give the probability density for two molecules to have an interaction energy ϵ. For the shell distribution at least one of the molecules is in the shell region, and for the bulk distribution at least one is in the bulk region.

Figure 10a shows that the shell water molecules have slightly fewer interactions in the −5 to −4 kcal/mol range and slightly more in the −3 to −1 kcal/mol range. The decrease in the strongly negative interactions is consistent with the slight decrease in numbers of hydrogen bonds for the shell region. The increase in weaker negative interactions compensates, giving essentially the same binding energy in the two regions. The distribution for the shell might be considered as indicating a *slight* decrease in structure for the shell. However, for comparison, in a study on the structure breaking effect of electrolytes, Geiger[32] showed that ions produce a much larger effect on these distributions than is shown here.

As previously mentioned, we are interested in delineating those urea-induced changes in the water–water interactions. The normalized distribution of water–water interactions (Figure 10b) for the shell has the same shape as the bulk distribution but lies below it. This is precisely what we would expect to observe if urea had no effect on water–water interactions: due to the presence of urea, water molecules in the shell region have fewer near-neighbor water molecules, which reduces the relative amplitude of the distribution in the strongly interacting regions. The difference in the distributions in Figure 10b may then be attributed simply to this difference.

The most interesting features of the pair interaction energy distributions arise from interactions among near-neighbor molecules. The large peak around zero is due to the many pairs of molecules which have small interactions because of their large separation. This peak may mask differences in near-neighbor interactions. With this in mind, we have also calculated near-neighbor or "local" pair interaction energy distributions which are shown in Figure 11. For these distributions water–water interactions are included only if the oxygen separation is less than 3.5 Å, and urea–water interactions are included only for waters in the shell region. The curves are all integrably normalized to unity so that the height of a curve is proportional to the probability that two molecules will have the corresponding interaction energy given that they meet the near-neighbor definitions employed. Figure 11b separates urea–water interactions from water–water interactions, as in Figure 10.

Figure 11a shows that in the shell region there is a decrease in the fraction of near neighbors with strong negative interactions ($\epsilon < -3$ kcal/mol), consistent with the data in Figure 10a, and an increase in the fraction with weak interactions (−2 kcal/mol

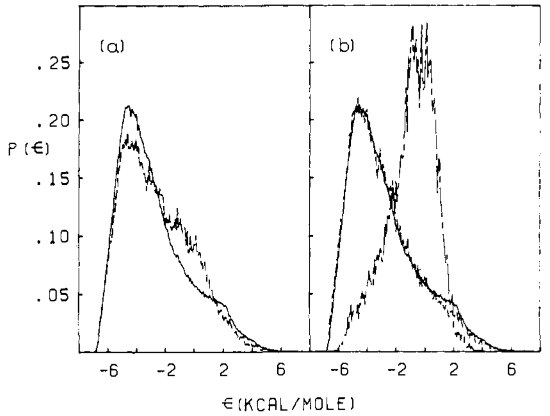

Figure 11. Normalized distributions of "local" pair interaction energies for water molecules; bulk (—). In (a), shell water–water and water–urea interactions (---); in (b) shell water–water interactions (---), shell water–urea interactions (– — -).

Table V. Average Numbers of H Bonds

	shell	bulk
	$\epsilon = -3$ kcal/mol	
$\langle n_{HB}^{T}\rangle$	2.93	3.02
$\langle n_{HB}^{W}\rangle$	2.79	3.02
$\langle n_{HB}^{U}\rangle$	0.14	0
	$\epsilon = 4$ kcal/mol	
$\langle n_{HB}^{T}\rangle$	1.95	2.02
$\langle n_{HB}^{W}\rangle$	1.90	2.02
$\langle n_{HB}^{U}\rangle$	0.05	0

$< \epsilon < 2$ kcal/mol) much of which is in fact masked by the huge peak in the earlier figure. The water–water distributions (Figure 11b) for the shell and the bulk are essentially identical. The presence of urea is *not* significantly perturbing the near-neighbor water–water interactions. This strongly supports our explanation of the differences in Figure 10b. The urea–water local interaction distribution, also shown in Figure 11b, is, however, markedly different from the water–water distribution. These results clearly show that the differences in pair energy distributions and hydrogen bond characteristics between the shell and bulk regions, evident in Figure 11a as well as earlier, are due to the direct interactions between urea and water and not a urea-induced perturbation of water–water interactions.

The most notable feature of the urea–water local pair interaction energy distribution is the broad maximum centered around zero, indicating that a large fraction of urea's near-neighbor water molecules have weak interactions with urea. The reason for this is evident from a comparison of the average number of nearest neighbors to the numbers of possible simultaneous hydrogen bonds. In the urea–water distribution an average of 12.6 water molecules are included while urea can reasonably be expected to form only 5 simultaneous hydrogen bonds with water.[39] Hence, a large fraction of the water molecules included as near neighbors to urea must have weak interactions with urea. For comparison, in the water–water distribution, a water molecule has an average of 5.49 near neighbors and 4 hydrogen bonding sites.

Since there are difficulties in obtaining consistent definitions of near neighbors for urea and water, the ratio of near neighbors to possible simultaneous hydrogen bonding sites may be somewhat exaggerated in the numbers above. For example, if one alternatively defines near neighbors as molecules whose heavy atoms (O, C, or N) are within 3.5 Å of each other, urea has 9.7 near-neighbor water molecules and ratios of near neighbors to simultaneous hydrogen bonds are 1.4 for water and 1.9 for urea. However, it is clear that any reasonable definition would show that this ratio is considerably higher for urea than water and consequently that a relatively large fraction of the near-neighbor water molecules will have weak interactions with urea.

Table VI. Urea–Water H Bonds

ε, kcal/mol	−4.0	−3.0	−2.0
total	0.685	1.51	2.98
proton acceptor	0.622	1.31	1.58
proton donor	0.063	0.38	1.40

Table VII. Percent of Saturation of H Bonds

ε, kcal/mol	−4.0	−3.0	−2.0
water	50.6	75.2	94.1
urea	13.7	30.2	54.6
proton acceptor	31.1	56.5	79.0
proton donor	2.1	12.7	46.7

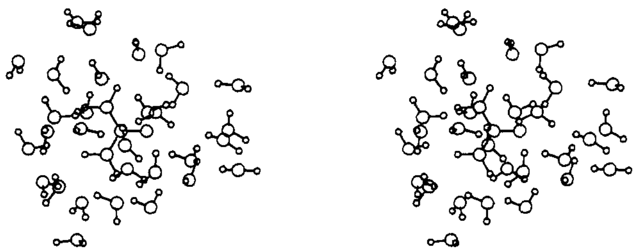

Figure 12. Stereographic view of urea and surrounding water molecules.

Urea–Water Hydrogen Bonding. We now consider the hydrogen bonding between urea and water. Table VI contains the numbers of hydrogen bonds between urea and water for three energetic definitions of a hydrogen bond. The hydrogen bonds are also separated into those in which urea acts either as a proton acceptor or as a proton donor, on the basis of whether the water's oxygen is closer to the urea oxygen (proton acceptor) or urea nitrogen (proton donor). The results show that the simulation manifests rather weak urea proton donor interactions; the majority have energeies between −2 and −3 kcal/mol.

A useful measure for the comparison of urea–water and water–water hydrogen bonding is a percent saturation. That is, we define percent saturation = (number of hydrogen bonds/number of possible simultaneous hydrogen bonds) × 100. In Table VI we list the percent saturation for water, urea, and the proton acceptor and donor bonds of urea at three energetic definitions of a hydrogen bond. The five possible simultaneous urea–water hydrogens consist of two in which urea acts as a proton acceptor and three as a proton donor. For the less stringent definitions of a hydrogen bond, there would be the possibility of including molecules which are not nearest neighbors but satisfy the energetic criterion. To avoid including these, for the present purposes, only pairs of water molecules whose oxygens are separated by less than 3.5 Å are considered for water–water hydrogen bonds, and only water molecules designated as shell are considered for urea–water hydrogen bonding.

The data in Table VII further indicates that the present calculation shows substantial hydrogen bonding between urea and water but that the degree of saturation is considerably less than for water–water hydrogen bonds. The weakness of urea's proton donor bonds is again apparent. It may be that these hydrogen bond characteristics are sensitive to the depths of the potential wells used for the urea–water interactions, and we have only qualitative information on these depths. For this reason, we cannot make a strong conclusion as to whether the water–urea interactions are, in fact, rather weak at the NH_2 site. Nevertheless, it should be noted that the minimum energy pairs (see Table III) are not very different among the sites. This fact supports the idea that the observed behavior is a result of the required water–urea bonding geometry and the competition of water–water interactions when many water molecules are present.

Dynamic Properties. As an additional test of the influence of urea on the surrounding water, we have compared self-diffusion coefficients and correlation functions for center of mass and angular velocities for the two regions. In all cases, there is no indication of significant differences between the shell and bulk regions. This is in contrast, for example, to aqueous electrolyte simulations,[32] where diffusion constants for the shell of about 1.5 times the bulk value are observed.

Stereographic Picture. In Figure 12 we show a stereoscopic view of urea and the surrounding water molecules for a representative configuration configuration from the simulation. The 30 water molecules closest to urea's center of charge are displayed. The tendency of the water molecules to orientate favorably with respect to both urea and other water molecules is apparent. As expected in a liquid, this configuration only faintly resembles that expected in a min*imum* energy configuration.[39]

IV. Discussion and Conclusions

Our simulation indicates that there are only small differences between water in the vicinity of urea and bulk water, and, furthermore, that these small differences are the result of direct interactions between urea and water molecules with no substantial urea-induced perturbation of water–water interactions. The quantities considered, including binding energies, pair interaction energy distributions, and hydrogen bonding, show that water molecules in the solvation shell of urea have properties which are very similar to those of bulk water.

Our results indicate that, in our judgment, urea has little effect on water structure, in contrast to the inference from several experiments that urea acts as a water structure breaker. The question, then, is whether an inconsistency exists. It is not feasible for us to calculate the relevant experimental quantities (such as NMR chemical shifts and ultrasonic and IR absorption) that have been used to indicate urea's structure breaking effect. However, the concept of "structural temperature" can be used as a bridge to compare different measures of structure and allow use to use experimental data to get a rough estimate of the magnitude of the differences we would expect to observe between the shell and bulk properties we have evaluated.

The structural temperature of an aqueous solution is the temperature at which pure water has the same value for the measured quantity as the solution. Both NMR proton chemical shifts[16] and infrared differential spectra[18] show approximately linear increases in structural temperature with urea concentration, up to 4 M urea, with slopes of about 1.7 K/M urea. Assuming the effect of urea is limited to shell region and using our mean shell occupancy, one finds that the structural temperature would have to be about 7 K higher than the bulk to account for this concentration dependence.

Mezei and Beveridge[8] have studied the effect of temperature on the measures of structure that are generally calculated in computer simulations of water. They found that the most sensitive measures were the radial distribution functions and the average number of hydrogen bonds per water molecule. The latter quantity is reported in our Table V. A comparison of the radial distribution functions for the shell and the bulk would be difficult to interpret due to the excluded volume effect of urea. However, the average number of hydrogen bonds for the two regions can be compared directly and the difference further compared to that change which a 7K rise in the temperature would produce in the bulk.

Using a geometric definition of hydrogen bond roughly equivalent to a −4 kcal/mol energetic cutoff for the ST2 model for water, Mezei and Beveridge calculated a decrease in the average number of hydrogen bonds per water molecule of 0.11 in going from 25 to 37 °C for Clementi's model for water (MCY). Assuming the decrease is linear with temperature over this range and that ST2 model manifests the same slope as MCY, which is adequate for the present purposes, a 7K rise in the shell structure temperature would correspond to an average number of hydrogen bonds per water molecule at −4 kcal/mol of 1.96 for the shell based on the bulk value of 2.02 found in the simulation. The value for the shell in the simulation is 1.95, almost exactly as predicted.

This close agreement must be in part fortuitous, and we do not consider this result as a verification of the accuracy of our simulation as compared to experiment. The calculation provides only a rough estimate, and the differences are small. However, we emphasize that the experiments indicate that we *should* expect to observe only very small changes in the water around urea, as we do. It is perhaps a matter of taste whether such changes should qualify urea as a structure breaker.

Regardless of whether one chooses to classify urea as a water structure breaker or not, it is difficult to imagine that changes in the water surrounding urea of the magnitude we observe in the simulation are responsible for urea's solubilization of hydrocarbons. We consider this to be a strong argument against the indirect mechanism, mentioned in the introduction, and feel that this solubilization most likely results from inclusion of urea in the solvation shell of the hydrocarbon. This will be examined in the following paper in this issue.

Note Added in Proof. The recent study of urea in water by Tanaka, Touhara, Nakanishi, and Watanabe[51] using an alternative set of interaction potentials manifests structural properties in close accord with those presented here.

Acknowledgment. Support of the work reported here by grants from the National Institute of General Medical Sciences (GM 30452) and the Robert A. Welch Foundation is gratefully achkowledged. P.J.R. is an Alfred P. Sloan Foundation Fellow and the Recipient of a Research Career Development Award (PHS Number CA00899) award by the National Cancer Institute, DHHS.

---

(51) Tanaka, H.; Touhara, H.; Nakanishi, K.; Watanabe, N. *J. Chem. Phys.* **1984**, *80*, 5170.